J Solid State Electrochem (2012) 16:1907–1915
DOI 10.1007/s10008-011-1588-0

ORIGINAL PAPER

Electrosynthesis of blue-light-emitting oligo(1-bromopyrene) with favorable solubility

Zhen Wang · Cunyuan Lai · Baoyang Lu · Wenjuan Guo · Ruirui Yue · Meishan Pei · Jingkun Xu

Received: 7 July 2011 / Revised: 30 October 2011 / Accepted: 2 November 2011 / Published online: 26 November 2011

Abstract Bromo-group-substituted oligopyrene films were electrochemically synthesized by direct anodic oxidation of 1-bromopyrene (BrP) in boron trifluoride diethyl etherate (BFEE). The oxidation potential of BrP was measured to be approximately 0.52 V (vs. Ag/AgCl), which was much lower than that detected in a neutral electrolyte such as acetonitrile (1.2 V vs. Ag/AgCl) and CH_2Cl_2 (1.25 V vs. Ag/AgCl). Oligo(1-bromopyrene) (OBrP) films showed good redox activity in both BFEE and concentrated sulfuric acid. Fourier transform infrared spectroscopy, ^{1}H NMR, and theoretical calculations showed that the electropolymerization of the BrP monomer mainly occurred at the $C_{(3)}$, $C_{(6)}$, and $C_{(8)}$ positions. As-formed OBrP was a typical blue light emitter with fluorescent quantum yields of 0.27, also emitted strong and bright blue photoluminescence at excitation of 365 nm UV light. Furthermore, the films were readily soluble in dimethyl sulfoxide, CH_2Cl_2, acetonitrile, and acetone. All these results indicate that the striking OBrP films have many potential applications in various fields, such as optoelectronic materials, DNA fluorescence probes, and electrochemical sensors.

Keywords Oligopyrene · Electrochemical polymerization · Blue-light-emitting · Conducting polymer

Z. Wang · C. Lai · W. Guo (✉) · M. Pei
School of Chemistry and Chemical Engineering,
University of Jinan,
Jinan 250022, China
e-mail: wzzzgj@126.com

B. Lu · R. Yue · J. Xu
Jiangxi Key Laboratory of Organic Chemistry,
Jiangxi Science and Technology Normal University,
Nanchang 330013, China

Introduction

Pyrene is an aromatic monomer with unique photophysical properties such as the long lifetime of its excited state, sensitivity toward micro-environmental changes, and propensity to p-stacking and also an important and thoroughly investigated organic chromophore. Therefore, pyrene and pyrene-based dyes are of increasing interest for these applications as a fluorescent probe for DNA base radicals, an indicator for bio-gas sensor and as a press-sensitive material [1, 2]. Oztekin et al. used glucose oxidase and poly-1,10-phenanthroline (PPMH) gained via electrochemical deposition to get the PPMH-modified GC electrode [3]. A pyrene label covalently attached to the sugar part of nucleosides has been used for the detection of nucleic acid hybridization [4–9]. Moreover, pyrene is a blue-emitting chromophore and has been proposed as a fluorescent temperature indicator. Some investigations were focused on using pyrene as an emitter for organic light-emitting diodes. On the other hand, oligopyrene is expected to possess better fluorescent and electroluminescent properties than those of pyrene monomer because of its longer delocalized p-electron chain sequence. And crystalline oligopyrene nanowires with multicolored emission have been also made by template-assisted electrochemical polymerization of the monomer pyrene [10].

Modification of the chemical structure by substitution of the pyrene unit has enabled synthesis of a large number of derivatives, resulting in numerous polymers with different degrees of stability, conductivity, solubility, and band gap. The bromine group on the main backbone can easily react with other compound, which will further improve the properties of inherently conducting polymers [11–13]. Then the introduction of the bromine group on the main

backbone of conducting polymers will also provide a novel approach for the functionalization of inherently conducting polymers. It is well-known that not all conducting polymers have fluorescence properties. Some compounds with poor fluorescence can react with 1-bromopyrene (BrP) to get good fluorescence property. On the contrary, some conducting polymers can be quenched their fluorescence with Ppy. It was reported that Ppy quenched the fluorescence of some fluorescent agents including fluorescein-5(6)-isothiocyanate (fluorescein), rhodamine B, and horseradish peroxidase by almost 100% when these fluorescent agents were adsorbed on the surface of Ppy [14].

It is well-known that electrochemical polymerization is a useful and widely applied technique for synthesizing conducting polymer (CP) films in common organic solvents, such as acetonitrile, CH_2Cl_2, or in water [15]. The CP films prepared by this technique are usually formed in an oxidized (doped) state and used without further treatment [16]. The doping levels of CP films depend strongly on the experimental conditions such as applied potential, electrolyte, supporting salt, and monomer structure [17]. The color and morphology of the CP films are known to change during the film growth process [18–20]. In recent years, boron trifluoride diethyl etherate (BFEE) has been found to be an excellent electrolyte for the electrochemical polymerization of aromatic compounds, such as benzene, thiophene, carbazole, fluorene, naphthalene, and their derivatives [21–27]. The interaction between the middle strong Lewis acid BFEE and the aromatic monomers lowers their oxidation potentials, and the catalytic effect of BFEE facilitates the formation of high-quality polymer films. Under these circumstances, BFEE serves not only as the solvent but also as the supporting electrolyte, and no other supporting electrolyte is needed. High-quality conducting polymer films can be created in BFEE.

In this paper, the electropolymerization of BrP (Scheme 1) in BFEE was studied. The electrochemical properties, thermal stability, fluorescence properties, and morphology of the as-prepared oligo(1-bromopyrene) (OBrP) films were studied in detail.

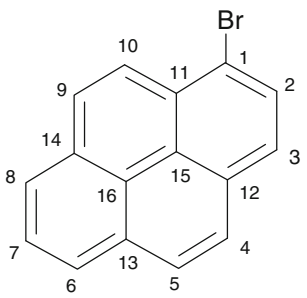

Scheme 1 Chemical structure of BrP

Experimental section

Materials

1-Bromopyrene (Alfa Aesar, 98%) was used as received. BFEE (Beijing Changyang Chemical Plant) was distilled and stored at −20°C before use. Sulfuric acid (98%), CH_2Cl_2, and 25% ammonia (Beijing Chemical Plant) were used without further purification. Commercial HPLC grade acetonitrile (ACN; made by Tianjin Guangfu Fine Chemical Research Institute, China) was used directly without further purification. Dimethyl sulfoxide (DMSO; analytical grade) was a product of Tianjin Bodi Chemicals Co. Ltd. Tetrabutylammonium tetrafluoroborate (TBATFB; Acros Organics, 95%) was dried in vacuo at 60 °C for 24 h before use. Other reagents were all analytical grade and used as received.

Electrosynthesis and electrochemical tests

Electrochemical polymerization and examination were performed in a one-compartment cell by the use of model 263 potentiostat–galvanostat (EG&G Princeton Applied Research) under computer control at room temperature. Electrochemical measurements were carried out with a platinum wire (diameter 0.5 mm) as working electrode. A stainless steel wire (diameter 1 mm) served as the counter electrode, and an Ag/AgCl electrode was used as the reference electrode. Stainless steel sheets with surface areas of 4 and 6 cm^2 were employed as the working and counter electrodes, respectively. The stainless steel sheets can be replaced by indium tin oxide (ITO) glass. Prior to each experiment, the electrodes were polished with abrasive paper (1500 mesh) except ITO. And all electrodes (including ITO) were cleaned with water and acetone successively and then dried in the air. The potentials mentioned in this paper refer to the Ag/AgCl electrode. The OBrP films were grown potentiostatically at 0.85 V vs. Ag/AgCl, and their thickness was controlled by the total charge passed through the cell, which was read directly from the current–time (*I–t*) curves by computer. After polymerization, the films were washed repeatedly with acetone to remove the electrolyte and monomer. For spectral analysis, OBrP films were dedoped with distilled 25% ammonia for 3 days. Finally, they were dried under vacuum at 60 °C for 24 h. And then, the film was scraped from the stainless steel sheet electrode and dissolved in adequate solvents for UV, Fourier transform infrared spectroscopy (FT-IR), ^1H NMR, thermogravimetric analysis (TGA), and fluorescence.

Characterizations

Infrared spectra were recorded using a Bruker Vertex 70 FT-IR spectrometer with samples in KBr pellets. The ^1H

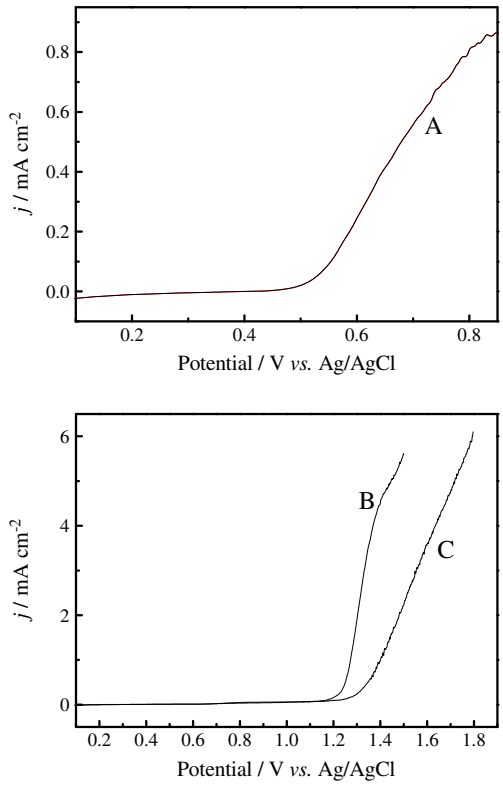

Fig. 1 Anodic polarization curves of 0.005 mol L^{-1}BrP on a platinum wire electrode in BFEE (*A*), ACN+0.1 mol L^{-1} TBATFB (*B*), and in CH_2Cl_2+0.1 mol L^{-1} TBATFB (*C*). Potential scan rates 50 mV s^{-1}

NMR spectra were recorded on a Bruker AV 400 NMR spectrometer with d_6-DMSO as the solvent and tetramethylsilane as an internal standard (singlet, chemical shift 0.0 ppm). Ultraviolet–visible (UV–vis) spectra were measured with a Perkin-Elmer Lambda 900 UV–vis near-infrared spectrophotometer. The fluorescence spectra were determined with an F-4500 fluorescence spectrophotometer (Hitachi). TGA was performed with a Pyris Diamond TG/DTA thermal analyzer (Perkin-Elmer). Scanning electron microscopy (SEM) measurements were made with a JEOL JSM-6360LA scanning electron microscope or a Cold Field Emission Electron Microscope S-4300 (Hitachi). The fluorescence quantum yields ($\phi_{overall}$) of PDPMF in solution was measured using anthracene in ACN (standard, ϕ_{ref}=0.27) as a reference and was calculated according to the well-known method given as Eq. 1

$$\phi_{overall} = \frac{n^2 A_{ref} I}{n_{ref}^2 A I_{ref}} \times \phi_{ref} \quad (1)$$

Here, n, A, and I denote the refractive index of solvent, the absorbance at the excitation wavelength, and the intensity of the emission spectrum, respectively. The subscript "ref" denotes the reference, and no subscript denotes the sample. Absorbance of the samples and the standard should be similar.

Results and discussion

Electrochemical study of the monomers

Figure 1 shows the anodic polarization curves of BrP in the electrolytes of pure BFEE (Fig. 1 A), ACN (Fig. 1 B), and CH_2Cl_2 (Fig. 1 C) containing 0.1 mol L^{-1} TBATFB, respectively, for comparison. It should be noted that BFEE is electrochemically stable in the whole potential range. The oxidation onset of BrP was initiated at 0.52 V vs. Ag/AgCl in pure BFEE (Fig. 1 A). The onset of oxidation increased to about 1.20 and 1.25 V vs. Ag/AgCl when the electrolyte was changed to ACN and CH_2Cl_2 (Fig. 1 B, C). This implies that the oxidation of BrP in pure BFEE is easier than that in ACN and CH_2Cl_2. Lower oxidation onset potentials of the monomer can prevent side reactions and lead to higher-quality OBrP films.

The electrochemical performances of the monomer were then examined by cyclic voltammetry in pure BFEE, ACN containing 0.1 mol L^{-1} TBATFB, and CH_2Cl_2 containing 0.1 mol L^{-1} TBATFB, respectively, as shown in Fig. 2. In

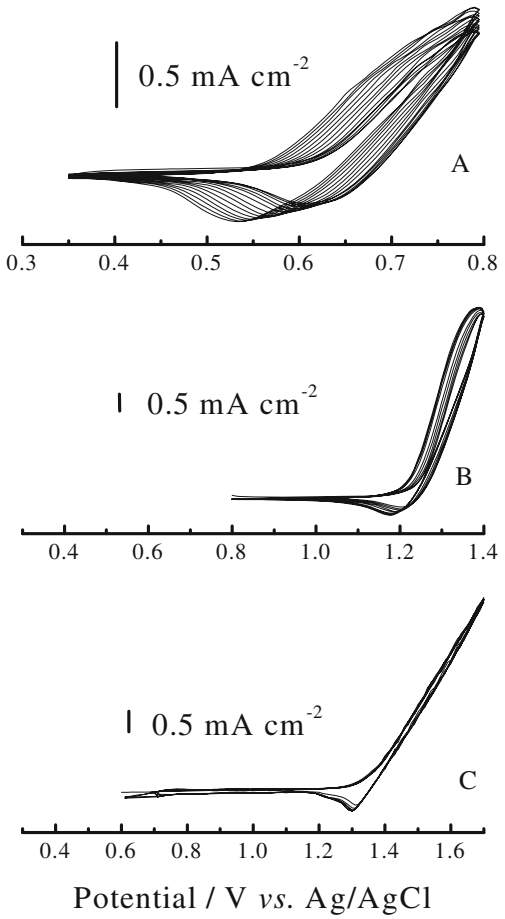

Fig. 2 Cyclic voltammograms of 0.005 mol L^{-1} BrP on a platinum wire electrode in BFEE (**A**), ACN+0.1 mol L^{-1} TBATFB (**B**), and in CH_2Cl_2+0.1 mol L^{-1} TBATFB (**C**). Potential scan rates 50 mV s^{-1}, potential scan cycles 10

ACN and CH_2Cl_2 (Fig. 2B, C), CVs are not satisfactory. No apparent redox waves were observed. Visual inspection during CV experiments revealed that there were no films formed on the working electrode surfaces, which may be attributable to the fair solubility of the oligomers in organic solvents like acetonitrile and methylene chloride. All of these implied that it was hard for BrP to deposit on the electrode in ACN-TBATFB or CH_2Cl_2-TBATFB by the potentiodynamic method, which also indicated that this method was not suitable for large-scale polymer deposition. The cyclic voltammetry of the monomer was also investigated in BFEE (Fig. 2A), an excellent electrolyte [28] in which many fused-ring compounds have been successfully electropolymerized [29–31]. The CVs of BrP in BFEE

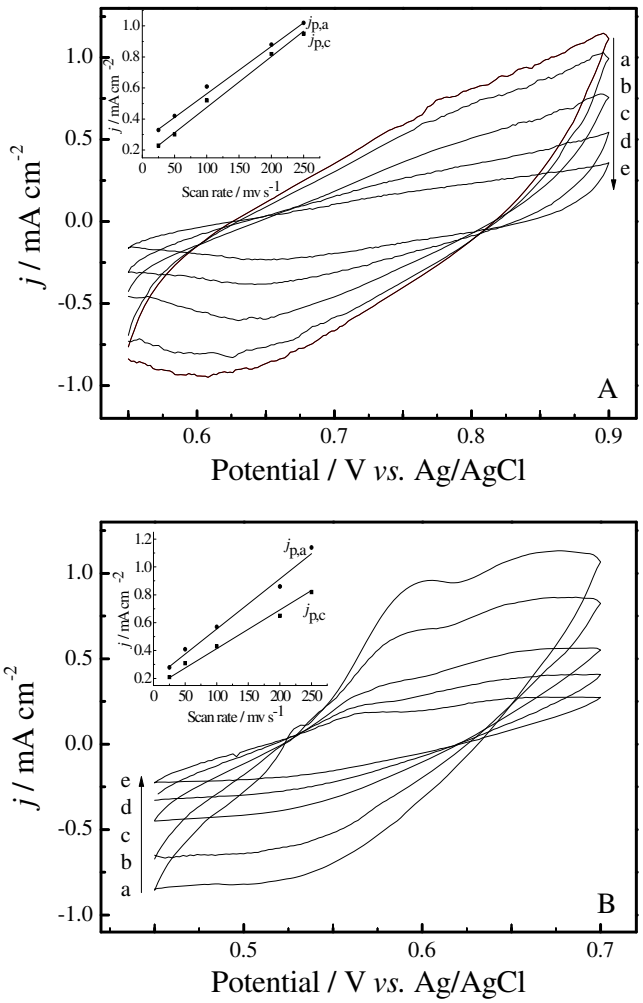

Fig. 3 Cyclic voltammograms of OBrP films on a platinum wire electrode in pure BFEE (**A**) and in concentrated sulfuric acid (**B**) at potential scan rates of 200 mV s^{-1} (*a*), 150 mV s^{-1} (*b*), 100 mV s^{-1} (*c*), 50 mV s^{-1} (*d*), and 25 mV s^{-1} (*e*). Polymer was synthesized potentiostatically at 0.85 V vs. Ag/AgCl in BFEE. *Inset*: plots of redox peak current densities vs. potential scan rates. j_p is the peak current density, and $j_{p,a}$ and $j_{p,c}$ denote the anodic and cathodic peak current densities, respectively

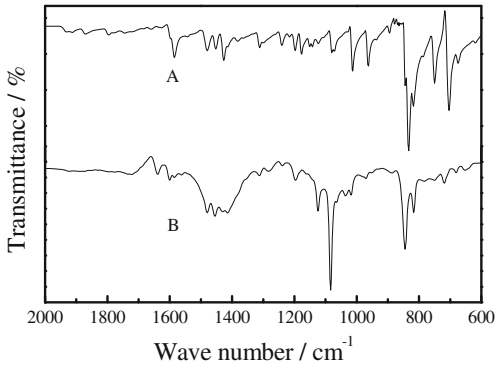

Fig. 4 FT-IR spectra of BrP monomer (*A*) and dedoped OBrP (*B*) prepared potentiostatically from BFEE

(Fig. 2A) show characteristic features of other conducting oligomers during potentiodynamic synthesis such as nitro-group-substituted pyrene [31] and pyrene [32]. The increase of redox peak currents in CVs implied that the amount of OBrP films increased on the electrode surface. The broad redox waves of the films may be ascribed to the wide distribution of OBrP chain length or the conversion of conductive species on the polymer main chain from the neutral state to polarons, from polarons to bipolarons, and finally from bipolarons to the metallic state [33]. All these phenomena indicate that BFEE was better than ACN and CH_2Cl_2 as the medium for the electrosynthesis of the conducting BrP.

Electrochemistry of OBrP films

In order to get a deeper insight into the electrochemical and environmental stability of as-formed polymer films and their electroactivity, the electrochemical behavior of OBrP films was determined carefully by cyclic voltammetry in monomer-free BFEE and concentrated sulfuric acid for comparison, as shown in Fig. 3. The peak current densities were proportional to the scanning rates (inset of Fig. 3A, B),

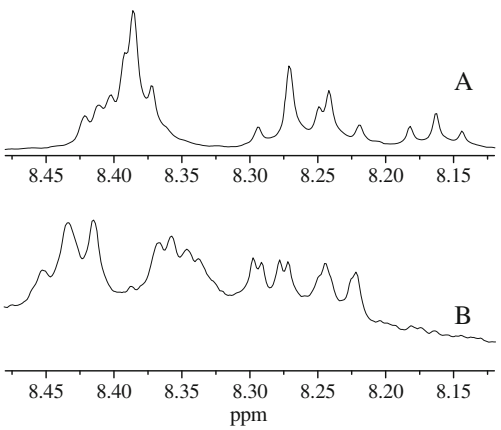

Fig. 5 ^{1}H NMR spectra of BrP (**A**) and OBrP (**B**) prepared potentiostatically from BFEE. Solvent: d_6-DMSO

Table 1 Main atomic electron-density populations for BrP

Atom	Electric charge
$C_{(1)}$	−0.031443
$C_{(3)}$	−0.163883
$C_{(5)}$	−0.131791
$C_{(7)}$	−0.078989
$C_{(9)}$	−0.134781
$C_{(11)}$	0.115551
$C_{(13)}$	0.122169
$C_{(15)}$	−0.002373
$C_{(2)}$	−0.083006
$C_{(4)}$	−0.129886
$C_{(6)}$	−0.158598
$C_{(8)}$	−0.158727
$C_{(10)}$	−0.123416
$C_{(12)}$	0.131134
$C_{(14)}$	0.127249
$C_{(16)}$	−0.011706

indicating a redox couple fixing on the electrode [34], and the redox processes are nondiffusional [27]. Furthermore, OBrP films could be cycled repeatedly between the conducting (oxidized) and the insulating (neutral) states without decomposition even in concentrated sulfuric acid, implying the good redox activity of OBrP films. The films could be oxidized and reduced from 0.85 V (anodic peak potential) to 0.57 V (cathodic peak potential) in monomer-free BFEE and from 0.67 to 0.50 V in concentrated sulfuric acid.

Structural characterizations

Figure 4 displayed the transmittance FT-IR spectra of BrP monomer (A) and dedoped OBrP obtained from BFEE. As seen from Fig. 4, the spectroscopy of OBrP was similar with that of BrP. The peaks located at about 1,426, 1,452, and 1,478 cm^{-1} were assigned to the stretching vibration of the C=C bond in the spectrum of the monomer (Fig. 4 A), which shifted to the broad peak at 1,415, 1,457, and 1,479 cm^{-1} for the oligomers (Fig. 4 B). Moreover, the bands in the region from 1,650 to 1,600 and 1,200 to 1,120 cm^{-1}were assigned to the stretching and shrinking modes of the C=C and C–C, which were selectively broadened in the OBrP (Fig. 4 B). The band at 1,084 cm^{-1} (Fig. 4 B) corresponded to the stretching vibration of the C–Br bonds in the benzene ring. This result implied that there was still bromine group on the dedoped OBrP backbone. The peaks at 885, 845, and 818 cm^{-1} in the oligomer spectrum reflected the 1,2,3,4,5-substituted and 1,2,3,4-substituted benzene ring, respectively. The absence of the 702-cm^{-1} peak and the emergence of an 885-cm^{-1} peak in the dedoped OBrP spectrum confirmed the electropolymerization of BrP [30]. However, the peaks in the spectrum of dedoped OBrP were not obviously broadened compared with those of the monomer, which is quite different from those of other conducting polymers [21–27] and may be attributable to the relatively short chain length of the as-formed OBrP.

To further investigate the polymer structure and the polymerization mechanism of BrP, ^{1}H NMR spectra of the monomers and the soluble dedoped OBrP were recorded in d_6-DMSO, as shown in Fig. 5. Compared with the monomers, the proton lines of OBrP were much broader than the corresponding proton lines of BrP monomer, probably due to a complex mixture of oligomers with different chain lengths. The wide molar mass distribution of polymer or the complex structure of the polymers led to slightly different environment of the atoms. For OBrP, the absence of the proton chemical shift at 8.38 and 8.14 ppm (Fig. 5B) indicated that BrP mainly electropolymerized through the coupling at $C_{(3)}$, $C_{(6)}$, and $C_{(8)}$ of the BrP. Although the spectrum of OBrP cannot provide distinct and lucid information about the structure of the oligomer, it confirmed the occurrence of the electrochemical polymerization among the monomers.

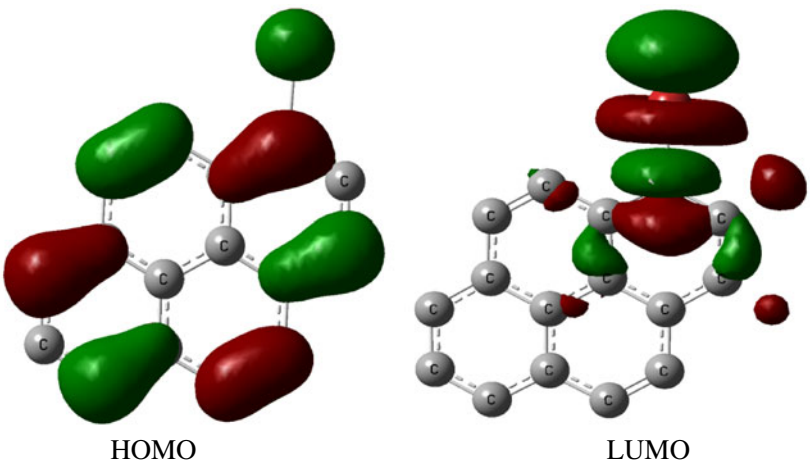

Scheme 2 Highest occupied molecular orbital (*HOMO*) and lowest unoccupied molecular orbital (*LUMO*) of BrP

Table 2 Main atomic electron spin densities for BrP

Atom	Electron spin density
$C_{(1)}$	0.230744
$C_{(3)}$	0.200172
$C_{(5)}$	0.108189
$C_{(7)}$	−0.103711
$C_{(9)}$	0.079460
$C_{(11)}$	−0.008778
$C_{(13)}$	−0.032165
$C_{(15)}$	−0.014177
$C_{(2)}$	−0.095559
$C_{(4)}$	0.066499
$C_{(6)}$	0.238242
$C_{(8)}$	0.229568
$C_{(10)}$	0.087606
$C_{(12)}$	0.003900
$C_{(14)}$	−0.016000
$C_{(16)}$	−0.002086

Quantum chemical calculations can provide some theoretical information on the chemical structure and property [35–37]. For more information on the structure of polymers and the polymerization mechanism, we calculated the atomic electron-density population (Table 1) and proportion of the frontier orbitals (Scheme 2) of the BrP monomers using the B3LYP/6-31G(d,p) level of Gaussian 03 software. In Table 1, the results of the main atomic electron-density populations revealed negative electric charges at the $C_{(3)}$, $C_{(4)}$, $C_{(5)}$, $C_{(6)}$, $C_{(8)}$, $C_{(9)}$, and $C_{(10)}$ positions in aromatic biphenyl, which implied that these atoms may donate electrons during electrochemical polymerization through radical cation intermediates. But the $C_{(3)}$, $C_{(6)}$, and $C_{(8)}$ positions have the more negative electric charges than $C_{(4)}$, $C_{(5)}$, $C_{(9)}$, and $C_{(10)}$ positions. According to the frontier molecular orbital theory, the reaction between the active molecules mainly happens on the highest frontier molecular orbitals. For BrP, the proportions of atoms at the $C_{(3)}$, $C_{(4)}$, $C_{(5)}$, $C_{(6)}$, $C_{(8)}$, $C_{(9)}$, and $C_{(10)}$ positions in the HOMO were

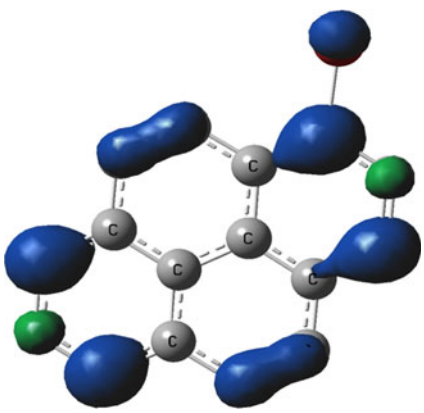

Scheme 3 Atomic electron spin densities of radical cation for BrP

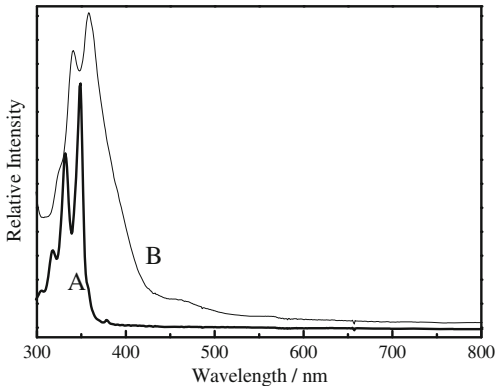

Fig. 6 UV–visible spectra of BrP (*A*) and dedoped OBrP (*B*) prepared from BFEE potentiostatically at 0.85 V vs. Ag/AgCl. Solvent: DMSO

higher than those of other atoms in Scheme 2. Meanwhile, the $C_{(3)}$, $C_{(6)}$, and $C_{(8)}$ positions also had rich negative charges. However, the electron spin density is the main factor in controlling the electropolymerization. Therefore, the monomer radical cation was calculated at the B3LYP/6-31 G(d,p) level for electron spin density [27, 29], and the isovalent surfaces of the electron spin density for these monomers are observed in Table 2 and Scheme 3. The relatively higher atomic electron density could be seen at the $C_{(3)}$, $C_{(6)}$, and $C_{(8)}$ positions, which implied that the electropolymerization of BrP probably occurs at these positions. Therefore, a reasonable conclusion can be easily drawn from all these theoretical results; that is, the polymerization between the monomer would happen preferentially on $C_{(3)}$, $C_{(6)}$, and $C_{(8)}$, well in accordance with FT-IR and ^{1}H NMR results mentioned previously.

UV–vis and fluorescence spectra

With the propagation of polymerization, some of the monomers became oligomer and then deposited on the

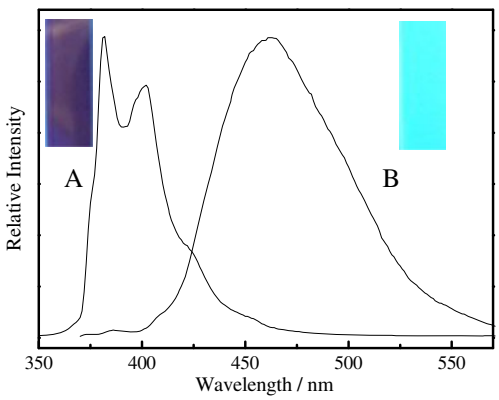

Fig. 7 The emission fluorescence spectra of BrP (*A*) and dedoped OBrP (*B*) deposited from BFEE potentiostatically at 0.85 V vs. Ag/AgCl. And photoluminescence of monomer (*A*) and OBrP (*B*) UV irradiation 365 nm (*inset*). Solvent: DMSO

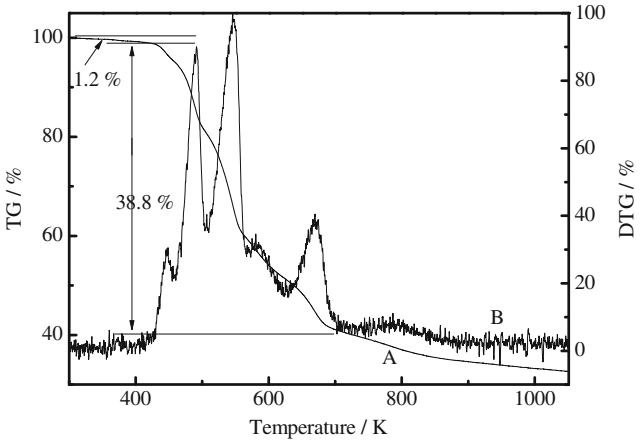

Fig. 8 TG (*A*) and DTG (*B*) curves of OBrP

electrode with the elongation of the main chain. However, some oligomers with short chain lengths still diffused from the electrode into the bulk solution. As a result, the bulk solution darkened progressively. The doped and dedoped OBrP were both soluble in common organic solvents such as acetone, ACN, DMSO, and CH_2Cl_2. Therefore, the UV–vis spectra of BrP, the dedoped OBrP dissolved in DMSO, were examined carefully, as shown in Fig. 6. BrP showed two characteristic absorption peaks at 330 and 349 nm (Fig. 6 A) which were assigned to a single electron π–π* transition of pyrene rings. It can be clearly seen that, due to the increase in the conjugated chain length, the overall absorption of the polymers tailed off to more than 358 nm for OBrP (Fig. 6 B). Moreover, the overall absorption of the oligomer tailed off to about 500 nm compared with that of the monomer (400 nm), which is mainly attributable to the increase in the conjugated chain length. Longer wavelengths in spectra usually indicate longer polymer sequence [38]. The spectral results confirmed the occurrence of electrochemical polymerization among the monomers and the formation of a conjugated polymer with broad molar mass distribution [30].

The fluorescence emission spectra of the monomers and the dedoped polymers were determined in DMSO, as shown in Fig. 7. The emission spectrum of BrP (Fig. 7 A) emerged at 381 nm, with a shoulder around 401 nm in DMSO, whereas a maximum emission peak at 461 nm characterized the spectrum of dedoped OBrP (Fig. 7 B). Large red shifts between the monomer and the polymer (about 60 nm) can be clearly seen from this figure, which can be ascribed to the elongation of the polymer's delocalized π-electron chain sequence. In this experiment, the fluorescence quantum yield of as-formed OBrP in DMSO was measured to be 0.27 according to Eq. 1, which was much higher than that of BrP (0.02). Meanwhile, it is also very interesting to find that soluble OBrP dissolved in common organic solvents, such as acetone, acetonitrile, and DMSO, can all emit strong blue photoluminescence when exposed to 365 nm UV light. Figure 7 (inset) shows the photoluminescence properties of soluble polymer when exposed to 365 nm UV light. As shown in Fig. 7 (inset A), soluble OBrP exhibited a bright blue-light-emitting property, whereas the monomer showed no emissions (Fig. 7, inset B). All the above results show that OBrP from the system is a typical blue light emitter, implying some potential applications in organic optoelectronics.

Thermal analysis

The thermal stability of OBrP is very important for potential application. For most conducting polymers, the

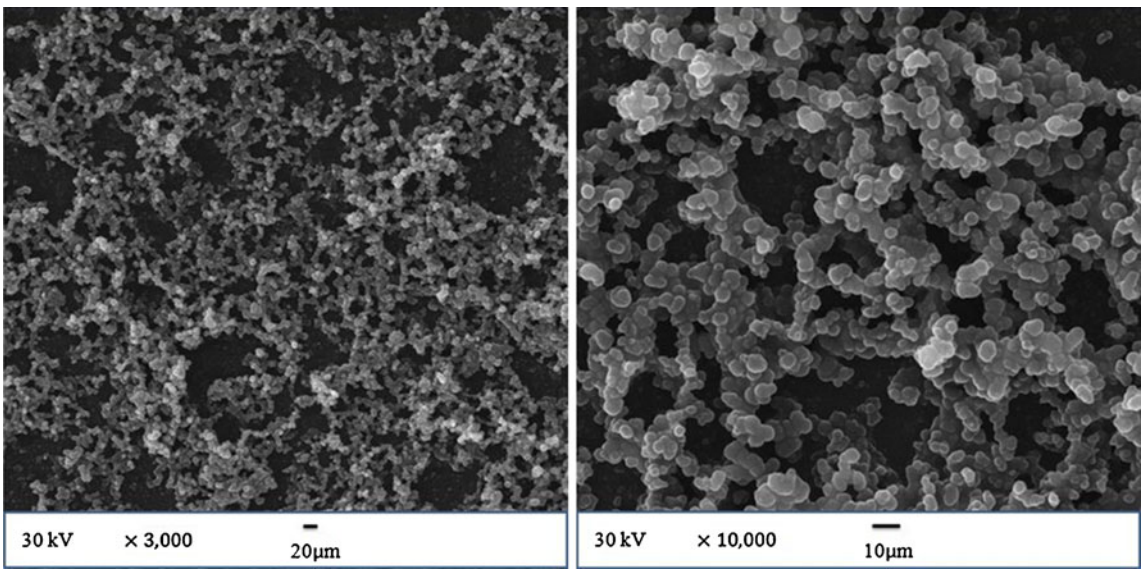

Fig. 9 Scanning electron micrographs of OBrP film electrodeposited on the glass electrode surface from pure BFEE potentiostatically at 0.85 V vs. Ag/AgCl

skeletal decomposition temperatures are usually low, generally reported to be lower than 600 K, which hinder their practical uses in various fields. To investigate the thermal stability of the newly obtained polymers, thermogravimetric analytical experiments were performed under a nitrogen stream. As shown in Fig. 8, it can be clearly observed that there were three-step weight losses for OBrP (Fig. 8 A). The polymer initially underwent a small weight decrease (about 1.2% for OBrP) from 300 to 415 K for OBrP, which may be attributed to water evaporation and other moisture or a few oligomers trapped in the polymer. With the gradual increasing of the temperature, a prominent weight loss step (about 38.8% for OBrP) was clearly found at 415 K$<T<$698 K, which were essentially due to the oxidizing decomposition of the skeletal OBrP backbone chain structures. The corresponding maximal decomposition of the polymers appeared at 491 and 547 K, respectively. The following degradation after 547 K was probably caused by the overflow of the oligomers decomposed from the polymer main chains, as mentioned previously. In addition, even when the temperature reached 1,000 K, the residual weight of the polymer films was 33.2%. These results indicated that the as-prepared OBrP films have high thermal stability, and their high decomposition temperatures indicate that they can be applied in a wide temperature scale, which is of special significance for some potential applications.

Morphology

The SEM images of the OBrP film electrodeposited on the glass electrode surface from pure BFEE was shown in Fig. 9. Microscopically, the OBrP film displayed sphere-type growth processes whereby a number of clusters were observed from Fig. 9. Moreover, this growth mode is a feature of stronger interactions between deposited molecules than between the film and substrate [27]. This morphology may facilitate the movement of doping anions into and out of the polymer film during doping and dedoping process, in good agreement with the higher redox activity of OBrP films and. This also confirmed the high-quality OBrP obtained in pure BFEE.

Conclusions

In summary, soluble OBrP films with excellent blue fluorescence were successfully electrosynthesized by direct anodic oxidation of its monomer BrP in BFEE. The oxidation potential of BrP in this medium was 0.52 V vs. Ag/AgCl. FT-IR spectra, ^{1}H NMR, and theoretical calculations showed that the electropolymerization of BrP occurred mainly at the $C_{(3)}$, $C_{(6)}$, and $C_{(8)}$ positions. The thermogravimetric results indicated good thermal stability of the as-prepared OBrP films. SEM images showed that sphere-type growth processes bromo-group-substituted oligopyrene was formed on the ITO electrode surface. With these good properties, OBrP may open up a potential area of research and hold promise for the design of new optoelectronic materials, electrochemical sensors, and probes.

Acknowledgments NSFC (50963002 and 51073074) and Key Laboratory of Photochemical Conversion and Optoelectronic Materials (TIPC, Chinese Academy of Sciences) are acknowledged for their financial support.

References

1. Huber R, Fiebig T, Wagenknecht HA (2003) Chem Commun 15:1878–1879
2. Basu BJ, Anandan C, Rajam KS (2003) Sensor Actuat B-Chem 94:257–266
3. Oztekin Y, Ramanavicienea A, Yazicigil Z, Solakc AO, Ramanaviciusa A (2011) Biosens Bioelectron 26:2541–2546
4. Yamana K, Zako H, Asazuma K, Iwase R, Nakano H, Murakami A (2001) Angew Chem 113:1138–1140
5. Korshun VA, Stetsenko DA, Gait MJ (2002) J Chem Soc Perkin Trans 18:1092–1104
6. Kawai K, Yoshida H, Takada T, Tojo S, Majima T (2004) J Phys Chem B 108:13547–13550
7. Kumar TS, Wengel J, Hrdlicka PJ (2007) ChemBioChem 8:1122–1125
8. Honcharenko D, Zhou C, Chattopadhyaya J (2008) J Org Chem 73:2829–2842
9. Nakamura M, Murakami Y, Sasa K, Hayashi H, Yamana K (2008) J Am Chem Soc 130:6904–6905
10. Qu LT, Shi GQ (2004) Chem Comm 24:2800–2801
11. Lo MY, Zhen CG, Lauters M, Jabbour GE, Sellinger A (2009) J Am Chem Soc 131:5718–5719
12. Printz M, Richert C (2009) Chem Eur J 15:3390–3402
13. Figueira-Duarte TM, Simon SC, Wagner M, Druzhinin SI, Zachariasse KA, Müllen K (2008) Angew Chem Int Ed 47:10175–10178
14. Ramanavicius A, Ryskevic N, Oztekin Y, Kausaite-Minkstimiene A, Jursenas S, Baniukevic J, Kirlyte J, Bubniene U, Ramanaviciene A (2010) Analytical Bioanalytical Chemistry 398:3105–3113
15. Diaz AF, Logan JA (1980) J Electroanal Chem 111:111–114
16. Roncali J (1992) Chem Rev 92:711–738
17. Sakamoto A, Furukawa Y, Tasumi M (1992) J Phys Chem 96:3870–3874
18. Downard AJ, Pletcer D (1986) J Electroanal Chem 206:147–152
19. Christensen PA, Hamentt A, Hillman AR (1988) J Electroanal Chem 242:47–62
20. Shi GQ, Xue G, Li C, Jin S, Yu B (1994) Macromolecules 27:3678–3679
21. Nie GM, Xu JK, Zhang SS, Han XJ (2006) J Appl Electrochem 36:937–944
22. Xu JK, Zhang YJ, Hou J, Wei ZH, Pu SZ, Zhao JQ, Du YK (2006) Eur Polym J 42:1154–1163
23. Lu BY, LI YZ, Xu JK (2010) J Electroanal Chem 643:67–76
24. Xu JK, Wei ZH, Du YK, Zhou WQ, Pu SZ (2006) Electrochim Acta 51:4771–4779

25. Wei ZH, Xu JK, Nie GM, Du YK, Pu SZ (2006) J Electroanal Chem 589:112–119
26. Lu BY, Xu JK, Li YZ, Liu CC, Yue RR, Sun XX (2010) Electrochim Acta 55:2391–2397
27. Lu BY, Yan J, Xu JK, Zhou SY, Hu XJ (2010) Macromolecules 43:4599–4608
28. Chen W, Xue G (2005) Prog Polym Sci 30:783–811
29. Nie GM, Han XJ, Zhang SS, Wei QL (2007) J Polym Sci Polym Chem 45:3929–3940
30. Lu BY, Xu JK, Fan CL, Jiang FX, Miao HM (2008) Electrochim Acta 54:334–340
31. Lu BY, Xu JK, Fan CL, Miao HM, Shen L (2009) J Phys Chem B 113:37–48
32. Lu GW, Shi GQ (2006) J Electroanal Chem 586:154–160
33. Chen XW, Inganals O (1996) J Phys Chem 100:15202–15206
34. Skotheim TA (ed) (1986) Handbook of conducting polymers. Marcel Dekker, New York
35. Zhang QZ, Yu WN, Zhang RX, Zhou Q, Gao R, Wang WX (2010) Environ Sci Technol 44:3395–3403
36. Xu F, Wang H, Zhang QZ, Zhang RX, Qu XH, Wang WX (2010) Environ Sci Technol 44:1399–1404
37. Zhang QZ, Li SQ, Qu XH, Shi XY, Wang WX (2008) Environ Sci Technol 42:7301–7308
38. Heather JB, Donald LG, William FM, Mark RP (1985) Makromol Chem 186:695–705